



Published in final edited form as:

Circ Arrhythm Electrophysiol. 2012 August 1; 5(4): 831–840. doi:10.1161/CIRCEP.111.969907.

Effect of SkM1 Sodium Channels Delivered Via a Cell Platform on Cardiac Conduction and Arrhythmia Induction

Gerard J.J. Boink, MSc^{1,3,4,*}, Jia Lu, PhD^{5,*}, Helen E. Driessen, BS¹, Lian Duan, MD¹, Eugene A. Sosunov, PhD¹, Evgeny P. Anyukhovskiy, PhD¹, Iryna N. Shlapakova, MD¹, David H. Lau, MD¹, Tove S. Rosen, MD^{1,2}, Peter Danilo, PhD¹, Zhiheng Jia, PhD⁵, Nazira Ozgen, MD, PhD¹, Yevgeniy Bobkov, BS¹, Yuanjian Guo, PhD⁵, Peter R. Brink, PhD⁵, Yelena Kryukova, PhD¹, Richard B. Robinson, PhD¹, Emilia Entcheva, PhD⁶, Ira S. Cohen, MD, PhD¹, and Michael R. Rosen, MD^{1,2,5}

¹Dept of Pharmacology, Center for Molecular Therapeutics, Columbia University, New York, NY ²Dept of Pediatrics, Columbia University, New York, NY ³Interuniversity Cardiology Institute of the Netherlands (ICIN), Utrecht ⁴Heart Failure Research Center, Academic Medical Center, University of Amsterdam, Amsterdam, the Netherlands ⁵Dept of Physiology & Biophysics, Institute for Molecular Cardiology, Stony Brook University, Stony Brook, NY ⁶Dept of Biomedical Engineering, Stony Brook University, Stony Brook, NY

Abstract

Background—In depolarized myocardial infarct epicardial border zones (EBZ), the cardiac sodium channel is largely inactivated, contributing to slow conduction and reentry. We have demonstrated that adenoviral delivery of the skeletal muscle sodium channel SkM1 to EBZ normalizes conduction and reduces induction of ventricular tachycardia/fibrillation (VT/VF). We now studied the impact of canine mesenchymal stem cells (cMSC) in delivering SkM1.

Methods and Results—cMSC were isolated and transfected with SkM1. Co-culture experiments showed cMSC/SkM1, but not cMSC alone, maintained fast conduction at depolarized potentials. We studied 3 groups in the canine 7d infarct: sham, cMSC and cMSC/SkM1. In vivo EBZ electrograms were broad and fragmented in sham, narrower in cMSC and narrow and unfragmented in cMSC/SkM1 ($P < 0.05$). During programmed electrical stimulation (PES) of EBZ, QRS duration in cMSC/SkM1 was shorter than in cMSC and sham ($P < 0.05$). PES-induced VT/VF was equivalent in all groups ($P > 0.05$).

Conclusions—cMSC provide efficient, effective delivery of SkM1 current. The interventions performed (cMSC or cMSC/SkM1) were neither antiarrhythmic nor proarrhythmic. Comparing outcomes with cMSC/SkM1 and viral gene delivery highlights the criticality of the delivery platform to SkM1 antiarrhythmic efficacy.

Keywords

arrhythmia; gene therapy; myocardial infarction; Na⁺ channels; cardiac conduction; cell therapy

Corresponding Author: Michael R. Rosen, MD, Gustavus A. Pfeiffer Professor of Pharmacology, Professor of Pediatrics, Director, Center for Molecular Therapeutics, Columbia University, 630 West 168 Street, PH 7W-321, New York, NY, 10032, Tel: 212-305-8754, Fax: 212-305-8351, mrr1@columbia.edu.

* contributed equally as first author

Conflict of Interest Disclosures: None.

Introduction

Reentry causes most life-threatening cardiac arrhythmias in ischemic heart disease.^{1,2} Antiarrhythmic drugs and surgery terminate reentrant arrhythmias by creating bidirectional conduction block, depressing conduction and/or prolonging refractoriness.³ Normalization of conduction in depressed pathways might be an antiarrhythmic alternative to blocking conduction. Yet, the only tools to affect such outcomes have been norepinephrine and acetylcholine, which hyperpolarize cell membranes and whose toxicities render their use here impractical.

We recently reported a novel means for speeding/normalizing conduction in settings associated with depolarized membrane potentials, leading to low availability of cardiac Na⁺ channels.^{4,5} The skeletal muscle Na⁺ channel (SkM1, Nav1.4) gene has a 10mV more depolarized midpoint of inactivation^{4,5} than the cardiac isoform (SCN5A, Nav1.5). Computer simulations indicated that SkM1 but not SCN5A expression preserves conduction velocity in depolarized environments.⁴ When administered via adenoviral vector into ventricular myocardium, SkM1 increases action potential (AP) V_{max} and conduction velocity and reduces the incidence of ventricular tachycardia/fibrillation (VT/VF) initiated by programmed electrical stimulation (PES) in healing infarcts⁴ or occurring spontaneously during ischemia/reperfusion.⁵

Because viral gene delivery is not innocuous, one objective of this study was to explore an alternative delivery system. We have successfully introduced HCN2, a pacemaker channel gene, into canine myocardium *in vivo* using adult human mesenchymal stem cells (hMSC) as a delivery platform. hMSC express cardiac connexins (Cx40 and Cx43⁶), electrically couple with myocytes and, carrying overexpressed HCN2 channels, create biological pacemakers in canine ventricle.⁷ These outcomes suggested feasibility of cell-based gene delivery. Therefore, we selected canine mesenchymal stem cells (cMSC) as a delivery platform in this study.

Preliminary *in vitro* experiments⁸ demonstrated superior effects of SkM1 over SCN5A on V_{max} and conduction in a cell line. We now report the isolation of cMSC, SkM1 properties in this delivery platform and their impact on conduction, arrhythmia induction, and AP V_{max} in healing canine infarcts.

Methods

Protocols were performed per American Physiological Society recommendations and reviewed and approved by the Columbia and Stony Brook University Institutional Animal Care and Use Committees.

Unless otherwise indicated, chemicals were from Sigma Chemical Co., St Louis, MO. An expanded version of the materials and methods and supporting data is provided in the online supplement.

Cell Isolation and Transfection

After euthanasia for other purposes, 4ml canine bone marrow was aspirated from the iliac crest of one year old dogs. cMSC isolation proceeded by standard techniques⁹, and transfection of the cells with SkM1 and SCN5A constructs was performed via electroporation using nucleofector technology (Amaxa Lonza, Gaithersburg, MD). Transfection efficiency was 30–45%.

In vitro studies

Whole cell patch clamp with a signal amplifier (Model Axopatch-1B, Axon Instruments Inc.) was used to measure single cell membrane current. Electrode resistances were 3–4 M Ω . The liquid junction potential (~8 mV between bath and electrode solutions) was not corrected because exchange between pipette and cell are never complete.¹⁰

Neonatal Sprague-Dawley rats were euthanized and ventricular myocytes isolated by an approved Stony Brook University IACUC protocol as previously described.¹¹ Isolated ventricular myocytes were re-plated at 4×10^5 cells/cm² for the control group and 3.5×10^5 cells/cm² for the coculture groups at a 20:1 ratio with cMSC onto grooved scaffolds. Cultures were maintained for 4–5 days before making functional measurements.

For immunocytochemistry, cMSC were loaded with quantum dots (Qdot 655, Invitrogen) before coculture. After 4 days coculture on plastic cover slips, samples were stained with mouse anti-connexin 43 (Invitrogen) and rabbit anti- α -actinin (Sigma), and then stained with Alexa 488 and Alexa 546 conjugated secondary antibodies (Invitrogen).

For functional measurements, scaffolds were washed and equilibrated at room temperature and stained with Fluo-4 AM (Invitrogen, Carlsbad, CA). A 2-D optical mapping system¹² was used to measure impulse propagation at room temperature.

Canine studies

cMSCs were prepared as above and used in passages 2–4. All batches employed had consistently high SkM1 sodium current expression in GFP-expressing cells. At the time of in vivo experimentation, cells were thawed, and trypan blue exclusion used to obtain % and total number of viable cells. 1×10^6 viable cells were suspended in 0.75 ml PBS. The percentage of viable cells was 70–90%.

Adult male mongrel dogs (22–25 kg; Chestnut Ridge Kennels, Chippensburg, Pa) were anesthetized with thiopental (17 mg/kg IV) and mechanically ventilated. Anesthesia was maintained with isoflurane (1.5–3.0%). A left thoracotomy was performed by sterile techniques, and coronary ligation performed as previously described.¹³ 1×10^6 cMSC were injected using a 23-gauge needle into three sites in the epicardial border zone (EBZ). The injection protocol was similar to that for adenoviral delivery.⁴ The chest was closed, lidocaine (50 $\mu\text{g} \cdot \text{kg}^{-1} \cdot \text{min}^{-1}$) was infused during surgery, and for 24–48h postoperatively. 7d later, dogs were anesthetized, the heart exposed, and ECGs and electrograms acquired, digitized, and stored on a personal computer (EMKA Technologies, Falls Church, Va).

Electrogram recordings, induction of ventricular tachycardia, microelectrode studies, infarct sizing, and immunohistochemistry were all performed as previously reported⁴ and are detailed in the online supplement.

Statistical Analysis

Data are expressed as mean \pm SEM. For *in vitro* studies, t-tests were used to compare between two groups and Kruskal-Wallis one way ANOVA followed by Dunn's multiple comparison test was used to analyze CV. Arrhythmia incidence in sham and cMSC or cMSC/SkM1-treated animals was analyzed by Fisher's exact test. ECG parameters, electrogram width recordings, and microelectrode data were analyzed using one way ANOVA followed by Bonferroni's post-tests. During PES at different cycle lengths, QRS duration was analyzed using two-way ANOVA for repeated measurements. $P < 0.05$ was considered significant.

The authors had full access to and take full responsibility for the integrity of the data. All authors have read and agree to the manuscript as written.

Results

Biophysical Comparison of SkM1 and SCN5A in cMSCs

To study voltage-dependent activation of SkM1 and SCN5A currents in GFP-positive cMSC (n=8/group), cells were held at -100 mV to prevent inactivation, and then pulsed to test potentials from -80 to $+40$ mV, with 5 mV increments (Figure 1A). SkM1 current started activating at -40 mV, was half maximal at -30 mV and peaked at -20 mV. Comparable SCN5A current measurements were -50 mV, t -40 mV and -25 mV respectively (Figure 1C). This suggests a 5 – 10 mV shift between activation of SkM1 and SCN5A channels. Reversal potentials were at 21.69 ± 1.87 mV and 21.09 ± 3.66 mV respectively; both close to the Nernst potential for Na^+ ($+23.31$ mV at 22°C). Peak current density and peak conductance density were 38.52 ± 4.74 pA/pF and 0.95 ± 0.14 nS/pF for SkM1, respectively and 55.09 ± 10.60 pA/pF and 1.27 ± 0.27 nS/pF for SCN5A, respectively. There were no significant differences in peak current density or peak conductance density between groups, suggesting comparable expression levels of both genes in cMSC.

To characterize steady-state SkM1 and SCN5A inactivation, cMSC were prepulsed for 500 msec to holding potentials from -100 mV to 0 mV, with 5 mV increments, and then stepped to 0 mV (Figure 1B). Normalized currents were fitted with the Boltzmann equation. SkM1 channel inactivation had a midpoint of -58.6 ± 0.4 mV, and slope factor of 6.0 ± 0.2 mV. SCN5A had a midpoint of -73.9 ± 0.1 mV and slope factor of 5.9 ± 0.1 mV (Figure 1D). Thus SCN5A inactivation was roughly 15 mV negative to SkM1 ($P < 0.05$). These data confirmed the relatively positive position of SkM1 inactivation voltage-dependence, suggesting cMSC/SkM1 may function better to deliver Na^+ current than cMSC/SCN5A in depolarized cells.

Similar to our HEK239 cells results,⁸ time constants for recovery from inactivation of SkM1 and SCN5A in cMSCs are smaller than those for SCN5A at all holding potentials (Supplementary Figure 4), especially at more depolarized potentials, suggesting much faster recovery of SkM1 in cMSC.

cMSC and cMSC/SkM1 Effects on *in vitro* Impulse Propagation

To confirm electrical coupling between cMSC and cardiac myocytes, we tested SkM1 effects on CV with cMSCs as the delivery system in the cocultures of myocytes and cMSC expressing SkM1 on PDMS scaffolds (Figure 2A–B). A linear Pt electrode was placed at one edge of the scaffold to pace at 1 Hz. Macroscopic optical mapping was carried out at room temperature to record propagation in 2-D. CV comparison among myocyte only, myocyte-cMSC, and myocyte-cMSC/SkM1 cocultures showed significantly higher CV in SkM1 cocultures in normal and high K^+ solutions (Figure 2C).

Studies in the Canine Model

Fourteen dogs were injected with cMSC, 10 with cMSC/SkM1, and 12 were not injected (sham). One cMSC animal died of VT 2 h after surgery. Two shams died of arrhythmias, one during surgery and one 2 d later. All cMSC/SkM1 animals survived. Animals that died in the first 2 d were excluded from further analysis. We performed terminal experiments at 7 d. During sinus rhythm, ECG cycle length, PR, QT and QTc did not differ among groups (Table 1A). However, QRS duration in cMSC and cMSC/SkM1 was shorter than sham ($P < 0.05$). Epicardial EBZ showed broad, fragmented electrograms (EGs) in sham; narrower EGs in cMSC and narrow, unfragmented EGs in cMSC/SkM1 (Table 1A, Figure 3).

ERP, QRS Duration and Arrhythmia Incidence during PES

ERP did not differ among groups (Table 1B). During PS site stimulation, QRS duration in cMSC and cMSC/SkM1 was shorter than sham ($P < 0.05$); and during EBZ site stimulation QRS duration was shorter in cMSC/SkM1 than cMSC or sham ($P < 0.05$; Figure 4). Despite the potentially therapeutic actions of cMSC/SkM1 on conduction, sustained VT/VF was induced in 7/10 cMSC/SkM1-injected dogs vs. 5/13 cMSC-injected dogs and 7/10 shams ($P > 0.05$).

Microelectrode studies

After the *in situ* protocol, tissue slabs of injected regions were used to study cMSC and cMSC/SkM1 impact on EBZ cellular electrophysiology. Resting membrane potential (RP) and AP duration (APD) did not differ among groups ($P > 0.05$; Table 1C). However, V_{max} in cMSC/SkM1 injected preparations was faster than sham and cMSC ($P < 0.05$; Table 1C). To provide further insight into the relation between V_{max} and membrane potential we plotted them against one another for all groups (Figure 5). This demonstrated that cMSC/SkM1 preparations have faster V_{max} over the full membrane potential range.

Infarct Size, Western Blotting and Histology

No differences in infarct size were seen among sham, cMSC and cMSC/SkM1 (29 ± 2.4 , 28 ± 2.1 , and $28 \pm 3.3\%$; $P > 0.05$). Western blotting indicated persistent presence of SkM1 protein in the injection site of cMSC/SkM1-injected animals whereas the non-injected site in these animals and all tested sites in cMSC or sham treated animals persistently showed absence of SkM1 protein (Figure 6A). Immunohistochemistry of cMSC/SkM1-injected regions demonstrated anti-Cx43 staining at the cMSC and adjacent myocardium interface (Figure 6B). SkM1/GFP-positive cMSC were not found in sham EBZ (Figure 6B).

Discussion

This study demonstrates: 1) SkM1 biophysical properties in cMSC are more favorable than SCN5A in restoring fast conduction in depolarized tissue, 2) cMSC/SkM1 but not unloaded cMSC maintain relatively fast conduction in depolarized tissue, 3) cMSC/SkM1-injected animals show prominent restoration of fast impulse propagation (narrow EGs, narrow prematurely-stimulated QRS complexes, and high V_{max} in excised tissue), 4) despite the potentially therapeutic actions of cellular SkM1 delivery there was no antiarrhythmic effect, contrasting with our previous work using viral delivery,⁴ 5) whereas prior literature suggests MSC may be proarrhythmic^{15,16}, we found MSC delivery to a healing canine infarct does not increase VT/VF incidence.

Biophysics of speeding conduction using cMSC-SkM1

Early work on circus movement arrhythmias,^{17,18} predicting cessation of reentry if conduction accelerated such that the activation wave front encountered its own refractory tail. Yet, initial pharmacological strategies to speed conduction (e.g. neurohormones) were hampered by proarrhythmia and limited success.² Novel drugs (rotigaptide and analogs)¹⁹ and gene therapies^{5,20} provided experimental means to speed conduction by enhancing gap junctional function, but their efficacy is still being debated^{21,22} and there are concerns that maintaining or increasing gap junctional function during acute infarction will increase infarct size.²⁰

Cell and gene therapies are being explored as means to prolong ERP and prevent reentry. Cell based strategies can induce post-repolarization refractoriness, but their antiarrhythmic efficacy is still under investigation.^{23,24} Prolonging repolarization and refractoriness is effective in monomorphic VT²⁵ and tachy-pacing induced AF;²⁶ efficacy against

polymorphic VT/VF is still unknown. Despite concerns regarding proarrhythmia accompanying local prolongation of repolarization, no proarrhythmia occurred in proof-of-concept studies.^{25,26}

Ischemic tissue is often depolarized, contributing to reduced Na-channel availability, slow conduction and reentry.^{27,28} Cardiac Na-channel inactivation is pivotal here,²⁹ and motivated our gene transfer of SkM1 channels whose inactivation kinetics favor current flow in depolarized tissue.^{4,5} These studies showed efficient restoration of conduction and protection against PES- or ischemia/reperfusion-induced arrhythmias.

Concerns regarding use of viral vectors led us to explore alternatives to viral gene transfer. Investigation of biophysical differences between SkM1 and the native cardiac Na-channel SCN5A in cMSC showed the midpoint of Na-channel inactivation shifted positively by 15 mV in SkM1- expressing cMSC as compared to cMSC expressing SCN5A – an outcome similar to results in HEK cells and NRVMs.^{8,30}

Approximately 60% of SkM1 channels are available at –60 mV contrasting with <10% of SCN5A channels. Other important predictors of sodium channel availability include fast inactivation and recovery from fast inactivation: both were accelerated in SkM1 vs. SCN5A. Together, these results suggest cellular SkM1 delivery should efficiently restore the pool of available sodium channels; in a fashion superior to cellular SCN5A delivery and to natively-available Na-channels.

Efficient coupling of delivery cells (here, cMSCs) to cardiac myocytes via gap junctions is central to ion current delivery. To this end, we previously reported that hMSC express Cx40 and Cx43 allowing efficient electrical coupling, delivery of overexpressed HCN2 current, and introduction of HCN2-based spontaneous activity in adjacent myocytes.^{6,31,32} In those studies, HCN2 current and spontaneous activity were blocked by carbonoxalone, highlighting the criticality of gap junctional coupling. To investigate the capability of cMSC/SkM1 to couple to myocytes and speed conduction we cocultured them with NRVMs. Cx43 was expressed at myocyte/cMSC interfaces and conduction velocities were increased in normal and depolarized conditions as compared to myocyte-only and myocyte/cMSC cell strands (Figure 2). This outcome encouraged our *in vivo* experiments.

Efficient and specific restoration of fast conduction in canine EBZ

One concern about the cMSC-based approach was the reduced pH of ischemic tissue, which results in closure of Cx43 gap junctions.^{33,34} This might limit the efficiency of SkM1 current delivery. Despite the potential for suboptimal coupling between myocytes and cMSCs, cMSC-SkM1 efficiently restored fast conduction in EBZ, as evidenced by: (1), local electrograms in EBZ were broad and fragmented in sham, narrow and less fragmented in cMSC, and narrow and unfragmented in cMSC-SkM1 (Figure 3); (2) QRS duration after application of PES in the EBZ was narrow in cMSC/SkM1-injected dogs, comparable to that of uninfarcted dogs. (3) QRS duration was shorter at normal and short coupling intervals – in cMSC/SkM1 dogs than in shams or those receiving cMSC (Figure 4); (4) V_{max} in isolated EBZ tissues of cMSC/SkM1 was significantly faster than in non-injected or cMSC-injected tissues (Figure 5). These results reflect restoration of fast inward Na current and speeding of conduction in EBZ by cMSC/SkM1 with efficiency comparable to that with viral SkM1.

Also similar to viral SkM1 delivery was the lack of proarrhythmia in hearts receiving cMSC/SkM1. Note as well that QT and QTc (Table 1A), ERP (Table 1B), and AP duration (Table 1C) were similar across groups, further illustrating that introducing SkM1 primarily impacts conduction without affecting repolarization. This suggests the outcomes of SkM1-based interventions arise from an effect on conduction.

Absence of protection against inducible VT/VF

Despite the efficacy of cMSC/SkM1 in restoring fast conduction in EBZ, protection against PES-induced VT/VF was not achieved. Several considerations might explain the absence of an antiarrhythmic effect:

First; the extent of speeding of conduction might be insufficient to prevent PES-induced VT/VF. This appears unlikely, as we previously demonstrated significant reduction in incidence of PES-induced VT/VF with a similar acceleration of conduction based on SkM1 gene transfer.⁴ We also showed SkM1 gene therapy speeds longitudinal conduction³⁵ and prevents ischemia/reperfusion-induced arrhythmias⁵, further supporting the notion that the extent of conduction speeding (similar to viral SkM1) should be antiarrhythmic.

Second; cMSCs could negatively impact conduction by acting as a current sink³¹ thereby slowing conduction and compensating the SkM1 effects. This is unlikely because unloaded cMSC did not slow conduction. In light of potential current sink effects, it should be noted that we use a small number of cells (~1 million) because we previously established this dose to generate significant ion channel-based biological function.⁷ This dose is much lower than that typically used in studies of cardiac regeneration (~200 million cells).^{36,37}

Third; prior research has shown that MSC form low resistance junctions but not intercalated disks with myocytes,⁶ Therefore, while conduction is sped by cMSC/SkM1, the organization needed for an antiarrhythmic effect may not be achieved. In addition it is possible that absence of intercalated discs in the cMSC-SkM1/myocyte unit supports formation and/or maintenance of reentrant pathways that otherwise would have remained incomplete.

Safety concerns of MSC-based therapies

When considering gene-modified or unmodified MSC transplantation as therapeutic approaches in cardiac disease two concerns have been extensively discussed: 1) the potential of MSC to be proarrhythmic³⁸ and 2) the risk for neoplasia.³⁹ The proarrhythmia concern is based on studies illustrating slowing of conduction and reentrant arrhythmias *in vitro*⁴⁰ and ERP shortening *in vivo*⁴¹ following MSC transplantation. However, other *in vivo* studies report absent^{42,43} or protective⁴⁴ effects with regard to ventricular arrhythmias. Our study supplements these findings by showing that transplanting a low dose of allogeneic MSC into the EBZ is safe and that it improves the conduction properties of the myocardium (Table 1A and Figure 4).

Concern for potential tumorigenesis resulting from MSC transplantation has primarily arisen because even early passage MSC can manifest chromosomal aberrations.⁴⁵ A murine model of MSC transplantation confirmed this concern.⁴⁶ Although a large body of literature suggests the use of human MSC is safe^{39,44}, recent reports of tumor formation in rodents⁴⁶ clearly warrant extensive safety analysis of MSC-based therapies.

Study limitations

In this study, we asked if cellular delivery of SkM1 protects against inducible arrhythmias 7 days post MI. We worked with a fixed end-point (1) because previous research indicated this provides a stable substrate for induction of reentrant arrhythmias²⁸ and (2) to allow direct comparison between cellular delivery of SkM1 and previously reported viral delivery.⁴ Furthermore, we only tested one dose of cells which had been highly effective in delivering electrical signals locally.⁷ Other experiments had indicated that 7 days is sufficient for MSCs to form gap junctions with myocytes and deliver ionic currents.³² We cannot exclude that a protocol using higher doses or later time points might have had a different outcome. Yet the outcome with the cellular approach - highly efficient normalization of conduction -

suggests that sufficient dose and time were available for cellular delivery of SkM1. The lack of specific antiarrhythmic effects of the cMSC/SkM1 intervention suggests that the cell delivery approach was complicated by the mechanistic problems discussed above rather than resulting from insufficient dose or time.

Conclusions

Using in vitro and in vivo approaches, we have shown cMSCs provide an efficient platform to control ion channel function in the vicinity of myocardial infarcts. We also have shown that effectiveness of SkM1-based antiarrhythmic therapy critically depends on the delivery vehicle, with viral gene delivery appearing superior. Further attempts to modify conduction in infarcted tissue may therefore be better focused on viral delivery of sodium channels, while cells might be reserved for myocardial repair.

Supplementary Material

Refer to Web version on PubMed Central for supplementary material.

Acknowledgments

Funding Sources: This work was supported by the National Heart, Lung and Blood Institute, HL094410, and New York State Department of Health, Stem Cell Contract CO24344. Gerard Boink received support from the Netherlands Heart Foundation, the Netherlands Foundation for Cardiovascular Excellence, the Dr. Saal van Zwabenberg foundation and the Interuniversity Cardiology Institute of the Netherlands.

References

1. Allesie MA, Boyden PA, Camm AJ, Kleber AG, Lab MJ, Legato MJ, Rosen MR, Schwartz PJ, Spooner PM, Van Wagoner DR, Waldo AL. Pathophysiology and prevention of atrial fibrillation. *Circulation*. 2001; 103:769–777. [PubMed: 11156892]
2. Wit AL, Janse MJ. Experimental models of ventricular tachycardia and fibrillation caused by ischemia and infarction. *Circulation*. 1992; 85:132–42. [PubMed: 1728503]
3. Janse MJ, Wit AL. Electrophysiological mechanisms of ventricular arrhythmias resulting from myocardial ischemia and infarction. *Physiol Rev*. 1989; 69:1049–1169. [PubMed: 2678165]
4. Lau DH, Clausen C, Sosunov EA, Shlapakova IN, Anyukhovskiy EP, Danilo P Jr, Kelly C, Duffy HS, Szabolcs MJ, Chen M, Robinson RB, Lu J, Kumari S, Cohen IS, Rosen MR. Epicardial border zone overexpression of skeletal muscle sodium channel SkM1 normalizes activation, preserves conduction, and suppresses ventricular arrhythmia: An in silico, in vivo, in vitro study. *Circulation*. 2009; 119:19–27. [PubMed: 19103989]
5. Anyukhovskiy EP, Sosunov EA, Kryukova YN, Prestia K, Ozgen N, Rivaud M, Cohen IS, Robinson RB, Rosen MR. Expression of skeletal muscle sodium channel (nav1.4) or connexin32 prevents reperfusion arrhythmias in murine heart. *Cardiovasc Res*. 2011; 89:41–50. [PubMed: 20823275]
6. Valiunas V, Doronin S, Valiuniene L, Potapova I, Zuckerman J, Walcott B, Robinson RB, Rosen MR, Brink PR, Cohen IS. Human mesenchymal stem cells make cardiac connexins and form functional gap junctions. *J Physiol*. 2004; 555:617–626. [PubMed: 14766937]
7. Plotnikov AN, Shlapakova I, Szabolcs MJ, Danilo P Jr, Lorell BH, Potapova IA, Lu Z, Rosen AB, Mathias RT, Brink PR, Robinson RB, Cohen IS, Rosen MR. Xenografted adult human mesenchymal stem cells provide a platform for sustained biological pacemaker function in canine heart. *Circulation*. 2007; 116:706–713. [PubMed: 17646577]
8. Lu J, Wang HZ, Jia Z, Zuckerman J, Lu Z, Guo Y, Boink GJJ, Brink PR, Robinson RB, Entcheva E, Cohen IS. Improving cardiac conduction with a skeletal muscle sodium channel by gene and cell therapy. *J Cardiovasc Pharmacol*. 2012 Epub ahead of print.
9. Pittenger MF, Mackay AM, Beck SC, Jaiswal RK, Douglas R, Mosca JD, Moorman MA, Simonetti DW, Craig S, Marshak DR. Multilineage potential of adult human mesenchymal stem cells. *Science*. 1999; 284:143–147. [PubMed: 10102814]

10. Mathias RT, Cohen IS, Oliva C. Limitations of the whole cell patch clamp technique in the control of intracellular concentrations. *Biophys J.* 1990; 58:759–770. [PubMed: 2169920]
11. Bien H, Yin L, Entcheva E. Calcium instabilities in mammalian cardiomyocyte networks. *Biophys J.* 2006; 90:2628–2640. [PubMed: 16399841]
12. Entcheva E, Bien H. Macroscopic optical mapping of excitation in cardiac cell networks with ultra-high spatiotemporal resolution. *Prog Biophys Mol Biol.* 2006; 92:232–257. [PubMed: 16330086]
13. le Marec H, Dangman KH, Danilo P Jr, Rosen MR. An evaluation of automaticity and triggered activity in the canine heart one to four days after myocardial infarction. *Circulation.* 1985; 71:1224–1236. [PubMed: 3888438]
14. Rosen AB, Kelly DJ, Schuldt AJ, Lu J, Potapova IA, Doronin SV, Robichaud KJ, Robinson RB, Rosen MR, Brink PR, Gaudette GR, Cohen IS. Finding fluorescent needles in the cardiac haystack: tracking human mesenchymal stem cells labeled with quantum dots for quantitative in vivo three-dimensional fluorescence analysis. *Stem Cells.* 2007; 25:2128–2138. [PubMed: 17495112]
15. Ly HQ, Nattel S. Stem cells are not proarrhythmic: letting the genie out of the bottle. *Circulation.* 2009; 119:1824–1831. [PubMed: 19349335]
16. Macia E, Boyden PA. Stem cell therapy is proarrhythmic. *Circulation.* 2009; 119:1814–1823. [PubMed: 19349334]
17. Mines GR. On dynamic equilibrium in the heart. *J Physiol.* 1913; 46:349–383. [PubMed: 16993210]
18. Mines GR. On circulating excitations in heart muscles and their possible relation to tachycardia and fibrillation. *Trans R Soc Can.* 1913; 46:349–383.
19. Hennen JK, Swillo RE, Morgan GA, Keith JC Jr, Schaub RG, Smith RP, Feldman HS, Haugan K, Kantrowitz J, Wang PJ, Abu-Qare A, Butera J, Larsen BD, Crandall DL. Rotigaptide (zp123) prevents spontaneous ventricular arrhythmias and reduces infarct size during myocardial ischemia/reperfusion injury in open-chest dogs. *J Pharmacol Exp Ther.* 2006; 317:236–243. [PubMed: 16344331]
20. Boink GJJ, Rosen MR. Regenerative therapies in electrophysiology and pacing: Introducing the next steps. *J Interv Card Electrophysiol.* 2010; 31:3–16. [PubMed: 21161675]
21. Macia E, Dolmatova E, Cabo C, Sosinsky AZ, Dun W, Coromilas J, Ciaccio EJ, Boyden PA, Wit AL, Duffy HS. Characterization of gap junction remodeling in epicardial border zone of healing canine infarcts and electrophysiological effects of partial reversal by rotigaptide. *Circ Arrhythm Electrophysiol.* 2011; 4:344–351. [PubMed: 21493965]
22. Wiegerinck RF, de Bakker JM, Opthof T, de Jonge N, Kirkels H, Wilms-Schopman FJ, Coronel R. The effect of enhanced gap junctional conductance on ventricular conduction in explanted hearts from patients with heart failure. *Basic Res Cardiol.* 2009; 104:321–332. [PubMed: 19139945]
23. Feld Y, Melamed-Frank M, Kehat I, Tal D, Marom S, Gepstein L. Electrophysiological modulation of cardiomyocytic tissue by transfected fibroblasts expressing potassium channels: a novel strategy to manipulate excitability. *Circulation.* 2002; 105:522–529. [PubMed: 11815438]
24. Yankelson L, Feld Y, Bressler-Stramer T, Itzhaki I, Huber I. Cell therapy for modification of the myocardial electrophysiological substrate. *Circulation.* 2008; 117:720–731. [PubMed: 18212286]
25. Sasano T, McDonald AD, Kikuchi K, Donahue JK. Molecular ablation of ventricular tachycardia after myocardial infarction. *Nat Med.* 2006; 12:1256–1258. [PubMed: 17072309]
26. Amit G, Kikuchi K, Greener ID, Yang L, Novack V, Donahue JK. Selective molecular potassium channel blockade prevents atrial fibrillation. *Circulation.* 2010; 121:2263–2270. [PubMed: 20479154]
27. Lue WM, Boyden PA. Abnormal electrical properties of myocytes from chronically infarcted canine heart. Alterations in V_{max} and the transient outward current. *Circulation.* 1992; 85:1175–1188. [PubMed: 1371431]
28. Ursell PC, Gardner PI, Albala A, Fenoglio JJ Jr, Wit AL. Structural and electrophysiological changes in the epicardial border zone of canine myocardial infarcts during infarct healing. *Circ Res.* 1985; 56:436–451. [PubMed: 3971515]

29. Pu J, Boyden PA. Alterations of Na⁺ currents in myocytes from epicardial border zone of the infarcted heart. A possible ionic mechanism for reduced excitability and postrepolarization refractoriness. *Circ Res.* 1997; 81:110–119. [PubMed: 9201034]
30. Protas L, Dun W, Jia Z, Lu J, Bucchi A, Kumari S, Chen M, Cohen IS, Rosen MR, Entcheva E, Robinson RB. Expression of skeletal but not cardiac Na⁺ channel isoform preserves normal conduction in a depolarized cardiac syncytium. *Cardiovasc Res.* 2009; 81:528–535. [PubMed: 18977767]
31. Potapova I, Plotnikov A, Lu Z, Danilo P Jr, Valiunas V, Qu J, Doronin S, Zuckerman J, Shlapakova IN, Gao J, Pan Z, Herron AJ, Robinson RB, Brink PR, Rosen MR, Cohen IS. Human mesenchymal stem cells as a gene delivery system to create cardiac pacemakers. *Circ Res.* 2004; 94:952–959. [PubMed: 14988226]
32. Valiunas V, Kanaporis G, Valiuniene L, Gordon C, Wang HZ, Li L, Robinson RB, Rosen MR, Cohen IS, Brink PR. Coupling an HCN2-expressing cell to a myocyte creates a two-cell pacing unit. *J Physiol.* 2009; 587:5211–5226. [PubMed: 19736302]
33. Penkoske PA, Sobel BE, Corr PB. Disparate electrophysiological alterations accompanying dysrhythmia due to coronary occlusion and reperfusion in the cat. *Circulation.* 1978; 58:1023–1035. [PubMed: 709759]
34. Garlick PB, Radda GK, Seeley PJ. Studies of acidosis in the ischaemic heart by phosphorus nuclear magnetic resonance. *Biochem J.* 1979; 184:547–554. [PubMed: 44193]
35. Coronel R, Lau DH, Sosunov EA, Janse MJ, Danilo P Jr, Anyukhovskiy EP, Wilms-Schopman FJ, Op't Hof T, Shlapakova IN, Ozgen N, Prestia K, Kryukova Y, Cohen IS, Robinson RB, Rosen MR. Cardiac expression of skeletal muscle sodium channels increases longitudinal conduction velocity in the canine 1-week myocardial infarction. *Heart Rhythm.* 2010; 7:1104–1110. [PubMed: 20385252]
36. Amado LC, Saliaris AP, Schuleri KH, St John M, Xie JS, Cattaneo S, Durand DJ, Fitton T, Kuang JQ, Stewart G, Lehrke S, Baumgartner WW, Martin BJ, Heldman AW, Hare JM. Cardiac repair with intramyocardial injection of allogeneic mesenchymal stem cells after myocardial infarction. *Proc Natl Acad Sci USA.* 2005; 102:11474–11479. [PubMed: 16061805]
37. Gyongyosi M, Blanco J, Marian T, Tron L, Petnehazy O, Petrasi Z, Hemetsberger R, Rodriguez J, Font G, Pavo IJ, Kertesz I, Balkay L, Pavo N, Posa A, Emri M, Galuska L, Kraitichman DL, Wojta J, Huber K, Glogar D. Serial noninvasive in vivo positron emission tomographic tracking of percutaneously intramyocardially injected autologous porcine mesenchymal stem cells modified for transgene reporter gene expression. *Circ Cardiovasc Imaging.* 2008; 1:94–103. [PubMed: 19808526]
38. Macia E, Boyden PA. Stem Cell Therapy Is Proarrhythmic. *Circulation.* 2009; 119:1814–1823. [PubMed: 19349334]
39. Williams AR, Hare JM. Mesenchymal stem cells: biology, pathophysiology, translational findings, and therapeutic implications for cardiac disease. *Circ Res.* 2011; 109:923–40. [PubMed: 21960725]
40. Chang MG, Tung L, Sekar RB, Chang CY, Cysyk J, Dong P, Marbán E, Abraham MR. Proarrhythmic potential of mesenchymal stem cell transplantation revealed in an in vitro coculture model. *Circulation.* 2006; 113:1832–1841. [PubMed: 16606790]
41. Price MJ, Chou CC, Frantzen M, Miyamoto T, Kar S, Lee S, Shah PK, Martin BJ, Lill M, Forrester JS, Chen PS, Makkar RR. Intravenous mesenchymal stem cell therapy early after reperfused acute myocardial infarction improves left ventricular function and alters electrophysiologic properties. *Int J Cardiol.* 2006; 111:231–239. [PubMed: 16246440]
42. Chen SL, Fang WW, Ye F, Liu YH, Qian J, Shan SJ, Zhang JJ, Chunhua RZ, Liao LM, Lin S, Sun JP. Effect on left ventricular function of intracoronary transplantation of autologous bone marrow mesenchymal stem cell in patients with acute myocardial infarction. *Am J Cardiol.* 2004; 94:92–95. [PubMed: 15219514]
43. Williams AR, Trachtenberg B, Velazquez DL, McNiece I, Altman P, Rouy D, Mendizabal AM, Pattany PM, Lopera GA, Fishman J, Zambrano JP, Heldman AW, Hare JM. Intramyocardial stem cell injection in patients with ischemic cardiomyopathy: functional recovery and reverse remodeling. *Circ Res.* 2011; 108:792–796. [PubMed: 21415390]

44. Hare JM, Traverse JH, Henry TD, Dib N, Strumpf RK, Schulman SP, Gerstenblith G, DeMaria AN, Denktas AE, Gammon RS, Hermiller JB Jr, Reisman MA, Schaer GL, Sherman W. A randomized, double-blind, placebo-controlled, dose-escalation study of intravenous adult human mesenchymal stem cells (prochymal) after acute myocardial infarction. *J Am Coll Cardiol.* 2009; 54:2277–2286. [PubMed: 19958962]
45. Ben-David U, Maysar Y, Benvenisty N. Large-scale analysis reveals acquisition of lineage-specific chromosomal aberrations in human adult stem cells. *Cell Stem Cell.* 2011; 9:97–102. [PubMed: 21816361]
46. Jeong JO, Han JW, Kim JM, Cho HJ, Park C, Lee N, Kim DW, Yoon YS. Malignant tumor formation after transplantation of short-term cultured bone marrow mesenchymal stem cells in experimental myocardial infarction and diabetic neuropathy. *Circ Res.* 2011; 108:1340–1347. [PubMed: 21493893]

In patients with a reduced ejection fraction the annual risk for sudden cardiac death in the healing phase after myocardial infarction is estimated to be as high as 10%. Ischemic heart disease is typically complicated by areas of membrane depolarization which inactivate cardiac sodium channels (encoded by SCN5a) and generate areas of slow conduction predisposing to reentrant arrhythmias. At present, available therapies for these arrhythmias are both limited and frequently ineffective. As a potential novel gene therapy we recently reported overexpression of the skeletal muscle sodium channel (SkM1). SkM1 channels are relatively resistant to inactivation by membrane depolarization and when overexpressed in the infarct epicardial border zone they were locally restored the speed of conduction and significantly reduced the incidence of induced ventricular tachycardia/fibrillation. As an alternative to the viral approach the present study investigated delivery of SkM1 channels via mesenchymal stem cells (MSCs). We found that MSCs couple to myocardium and can be safely administered to the depolarized epicardial border zone. We also found that SkM1 loaded MSCs efficiently deliver sodium current and restore the speed of impulse propagation. Yet despite these potentially therapeutic outcomes and in contrast to the viral approach, cellular delivery of SkM1 appeared not to be antiarrhythmic thus indicating the criticality of the delivery platform in obtaining the antiarrhythmic effect. No proarrhythmia occurred. Future SkM1-based antiarrhythmic approaches should therefore focus on viral delivery.

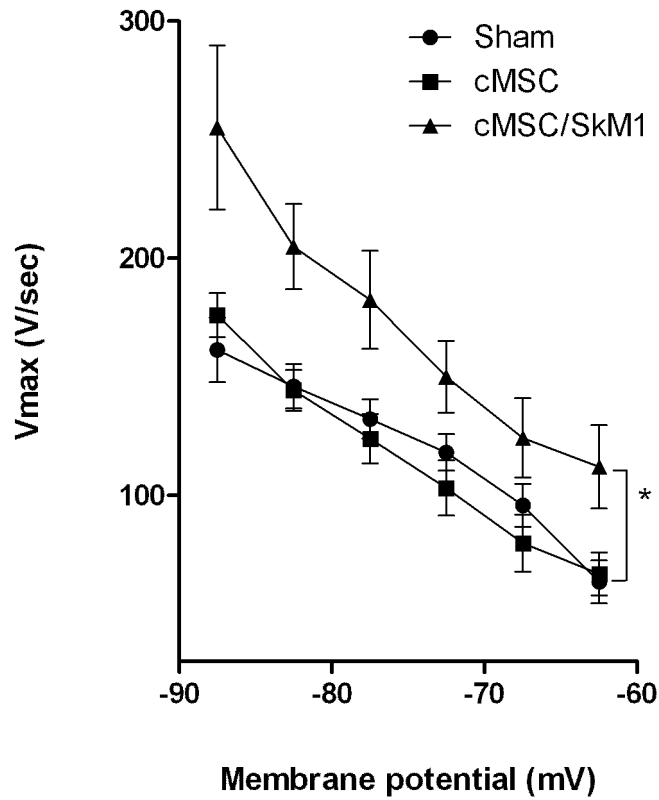


Figure 1.

SkM1 and SCN5A expression in cMSCs. **A**, SkM1 and SCN5A activation in cMSCs held at -100 mV and then pulsed to test potentials from -80 mV to $+40$ mV, per Methods. **B**, Inactivation of SkM1 and SCN5A currents in cMSCs held at potentials from -100 mV to 0 mV with 5 mV increments. **C**, Current-voltage relationship of SkM1 ($n=8$) and SCN5A ($n=8$) in cMSCs, normalized to maximum peak current. **D**, Inactivation curve (the h_{∞} curve) of SkM1 ($n=8$) and SCN5A ($n=8$). Data are normalized to the maximum peak current and fit

to the Boltzmann equation $f = \frac{1}{1 + \exp[(E_m - V_h)/K]}$, where V_h is the midpoint membrane potential and K is the slope factor.

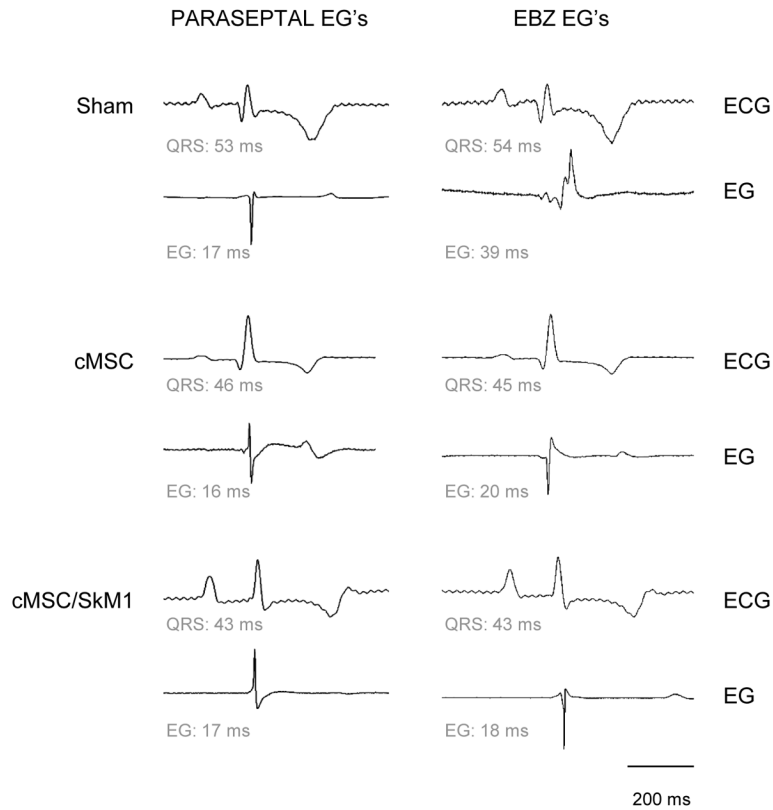


Figure 2.

Effect of cMSC/SkM1 on CV in *in vitro* cardiac syncytium. **A–B**, According previously described methods¹⁴, cMSCs were loaded with quantum dots (red) before being cocultured with myocytes. Cultures were fixed and stained 4 days after initiation of coculture. Nuclei were counterstained using DAPI (blue). **A**, Low amplification micrographs showing the distribution of QDs loaded cMSCs (red) in relation to the cultured myocytes stained for Cx43 (green); scale bar represents 40 μ m. **B**, High amplification micrographs showing Cx43 expression (green) at the interface (yellow arrows) between myocytes (stained orange for α -actinin) and cMSCs loaded with quantum dots (red); scale bar represents 10 μ m. **C**, Comparison of CV in myocyte-only (n=33), myocyte-cMSC (n=17) and myocyte-cMSC/SkM1 (n=28) cultures in normal and high K Tyrode's (* P <0.05).

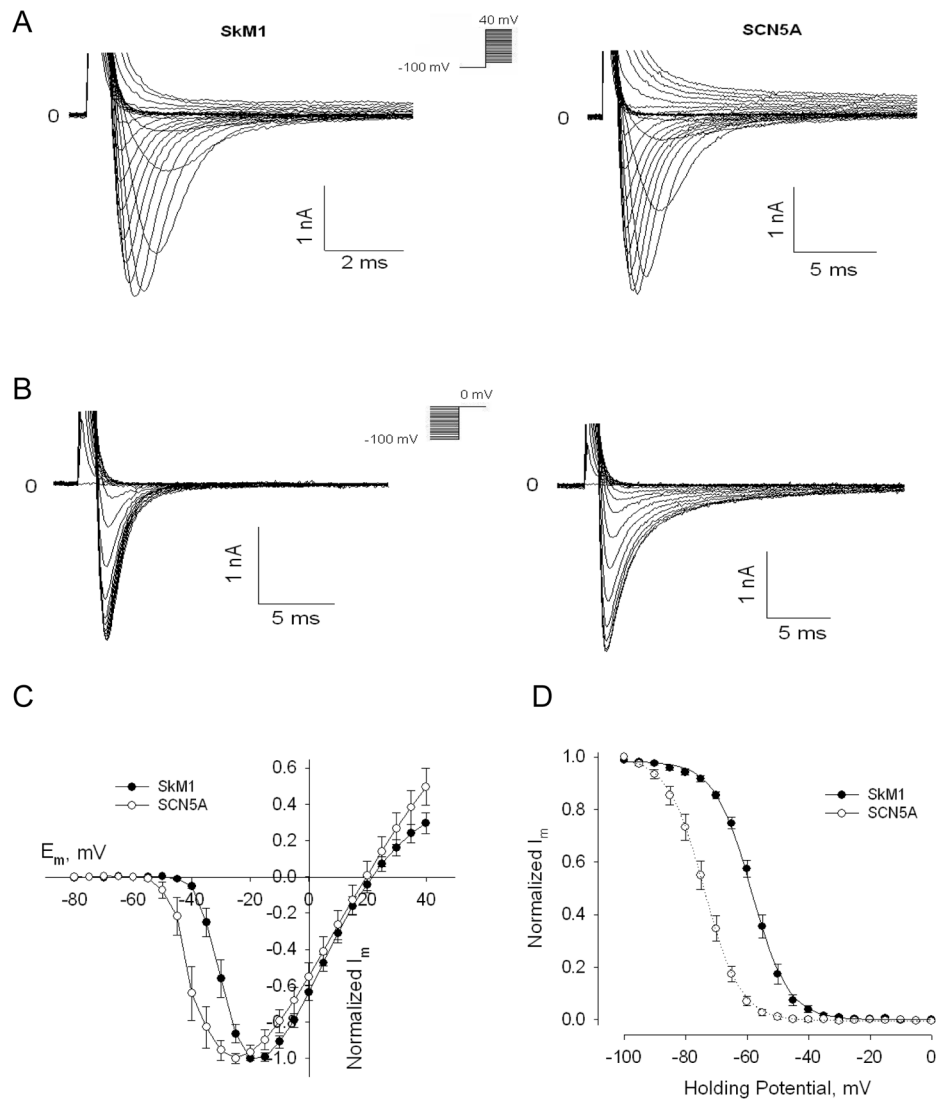


Figure 3. Typical recordings of lead II ECG (upper) and local electrograms (lower) - in normal myocardium (left) and EBZ; right.

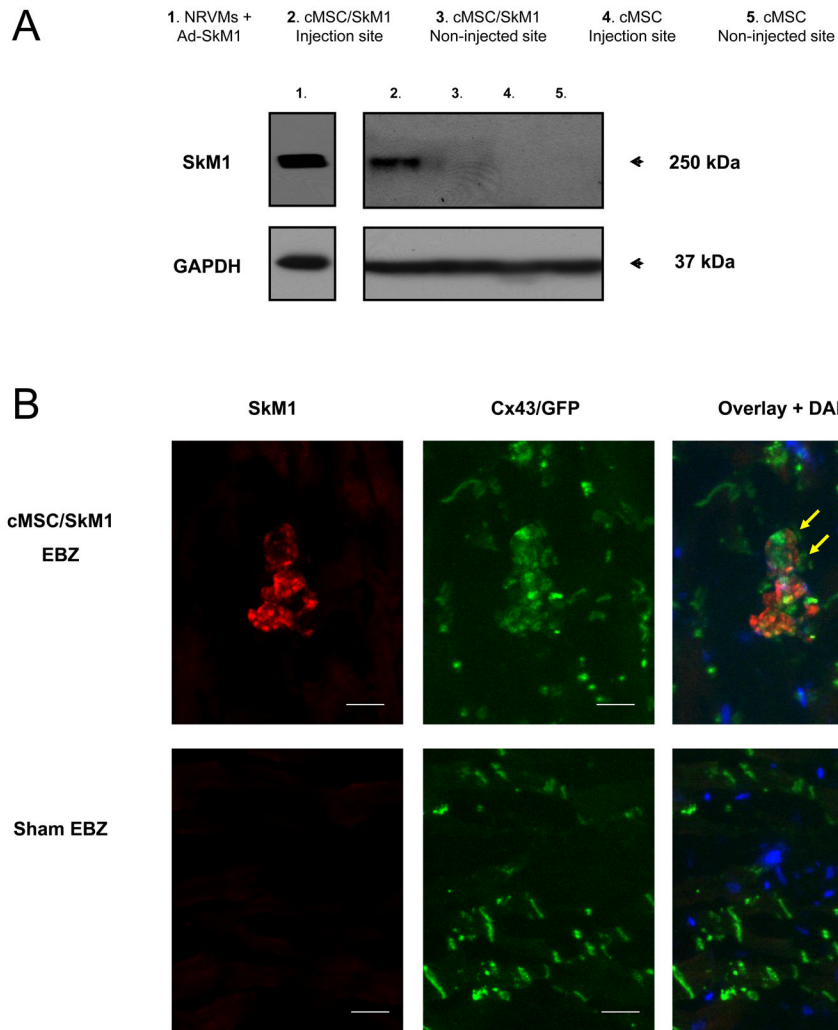


Figure 4.

QRS duration during normal and premature stimulation. QRS duration during stimulation from the paraseptal (PS; left) and EBZ/injection (right) regions. Note shorter QRS duration in cMSC/SkM1-injected animals ($*P < 0.05$). Electrical stimulation applied per Methods. Some animals could not be included in this analysis because they fibrillated before completing the protocol (PS; Sham n=7, cMSC n=12, cMSC/SkM1 n=9, and EBZ; Sham n=5, cMSC n=9, cMSC/SkM1 n=8).

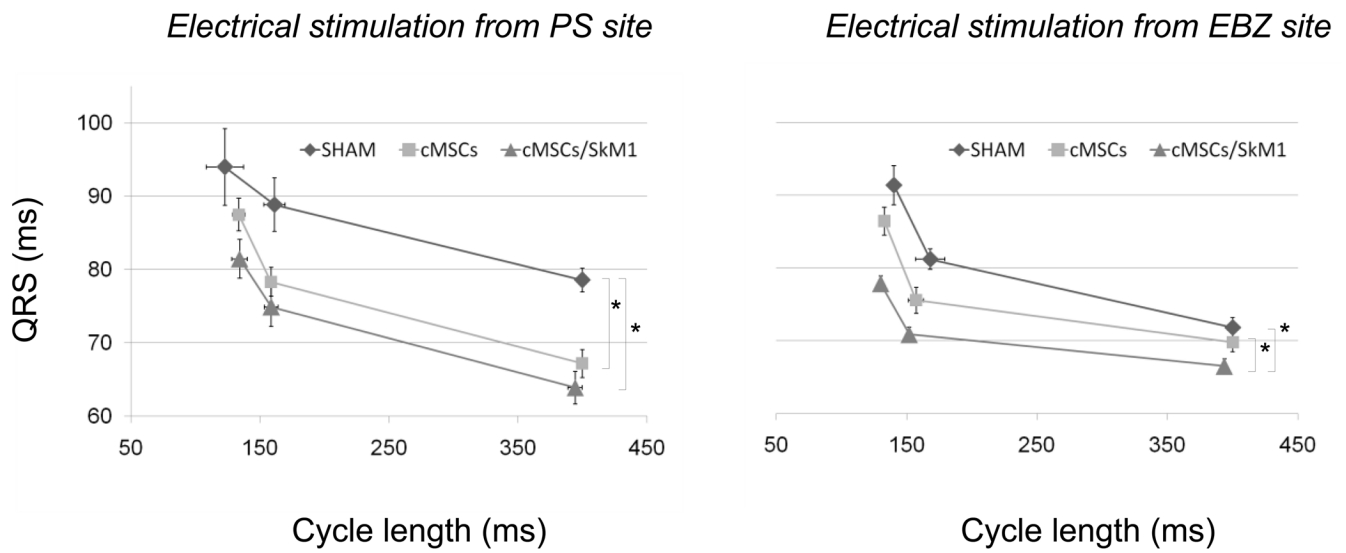


Figure 5. Action potentials have higher membrane responsiveness (V_{max} vs. MP) curves in cMSC/SkM1 injected preparations vs. Sham and cMSC (*; $P < 0.05$).

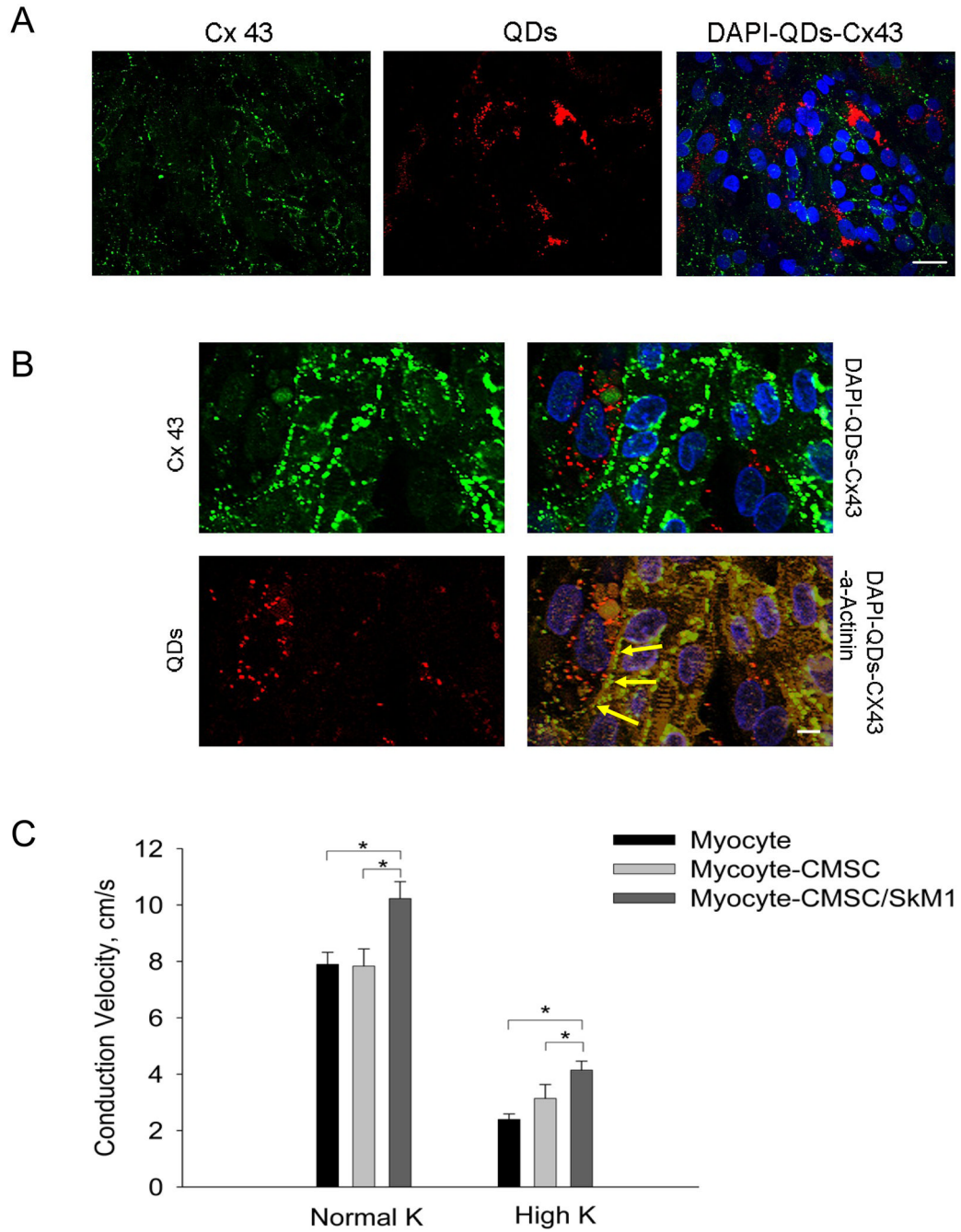


Figure 6.

Western blotting and immunohistochemistry of EBZ. **A**, Western blotting of injection site samples from cMSC/SkM1-treated animals showed a specific positive band at 250 kDa comparable to the signal obtained from virally transduced (using an SkM1 adenovirus; Ad-SkM1) neonatal rat ventricular myocytes (NRVMs) that were used here as a positive control. This 250 kDa SkM1-specific signal was not obtained in tissue from non-injected EBZ of cMSC/SkM1-treated animals nor was it obtained from sham (not shown) or cMSC-treated animals. GAPDH was used as a loading control. **B**, In cMSC/SkM1 injected cells, coimmunohistochemical experiments showed Cx43 (green) on the interface (yellow arrows)

between myocardium and SkM1 positive cells. GFP is visualized via direct fluorescence (green) and not optometrically separated from the Cx43 signal. SkM1 positive cells were not detected in sham. Nuclei were counter-stained (blue) using DAPI. Bar=25 μ m.

Table 1A

ECG and local electrogram (EG) measurements during sinus rhythm. Note that only the local EG duration in anterior wall of the left ventricle (LV) – the injected epicardial borderzone (EBZ) – differs among groups. PS: paraseptal site.

Measurement	Sham	cMSC	cMSC/SkM1
ECG parameters, ms			
Cycle length	567±37.2	562±30.1	560±33.6
PR	96±4.4	98±4.3	100±3.5
QRS	56±1.4	47±2.4 *	44±1.2 *
QT	220±5.6	207±5.5	210±7.9
QTc	294±4.8	277±6.5	282±5.7
EG duration, ms			
LV basal (PS)	21±0.8	22±1.3	21±2.1
LV anterior (EBZ)	32±1.9	26±1.4 *	21±1.6 †
RV anterior	22±1.1	20±0.4	21±0.8

Sham n=10, cSMC n=13, cMSC/SkM1 n=10.

* : $P < 0.05$ vs. Sham,

† : $P < 0.05$ vs. cMSCs and Sham.

Table 1B

Effective refractory period (ERP) recorded during PES from the paraseptal region (PS) and from the EBZ/
injection region.

Measurement	Sham	cMSC	cMSC-SkM1
ERP (PS), ms	168±2.8	157±4.4	163±5.3
ERP (EBZ), ms	167±4.2	158±4.8	153±4.0

Sham n=10, cSMC n=13, cMSC/SkM1 n=10.

Table 1C*In vitro* electrophysiological parameters recorded from EBZ tissues.

Measurement	Sham	cMSC	cMSC-SkM1
MDP, -mV	78.2±1.6	77.9±1.1	78.5±1.6
V _{max} , V/S	157.8±10.4	148.0±8.0	201.0±13.9 †
APD30, ms	38.7±7.4	43.9±4.8	49.6±8.1
APD50, ms	54.9±8.6	70.0±7.3	74.8±11.5
APD90, ms	87.3±9.1	109.9±8.6	113.2±12.9

†: $P < 0.05$ vs. cMSCs and Sham.

Sham n=10, cSMC n=13, cMSC/SkM1 n=10.